

Video Article

Thinned-skull Cortical Window Technique for *In Vivo* Optical Coherence Tomography Imaging

Jenny I. Szu¹, Melissa M. Eberle², Carissa L. Reynolds², Mike S. Hsu¹, Yan Wang², Christian M. Oh², M. Shahidul Islam², B. Hyle Park², Devin K. Binder¹

¹Division of Biomedical Sciences, University of California, Riverside

²Department of Bioengineering, University of California, Riverside

Correspondence to: Devin K. Binder at dbinder@ucr.edu

URL: <http://www.jove.com/video/50053>

DOI: [doi:10.3791/50053](https://doi.org/10.3791/50053)

Keywords: Neuroscience, Issue 69, Bioengineering, Medicine, Biomedical Engineering, Anatomy, Physiology, Thinned-skull cortical window (TSCW), Optical coherence tomography (OCT), Spectral-domain OCT (SD-OCT), cerebral cortex, brain, imaging, mouse model

Date Published: 11/19/2012

Citation: Szu, J.I., Eberle, M.M., Reynolds, C.L., Hsu, M.S., Wang, Y., Oh, C.M., Islam, M.S., Park, B.H., Binder, D.K. Thinned-skull Cortical Window Technique for *In Vivo* Optical Coherence Tomography Imaging. *J. Vis. Exp.* (69), e50053, doi:10.3791/50053 (2012).

Abstract

Optical coherence tomography (OCT) is a biomedical imaging technique with high spatial-temporal resolution. With its minimally invasive approach OCT has been used extensively in ophthalmology, dermatology, and gastroenterology¹⁻³. Using a thinned-skull cortical window (TSCW), we employ spectral-domain OCT (SD-OCT) modality as a tool to image the cortex *in vivo*. Commonly, an opened-skull has been used for neuro-imaging as it provides more versatility, however, a TSCW approach is less invasive and is an effective mean for long term imaging in neuropathology studies. Here, we present a method of creating a TSCW in a mouse model for *in vivo* OCT imaging of the cerebral cortex.

Video Link

The video component of this article can be found at <http://www.jove.com/video/50053/>

Introduction

Since its introduction in the early 1990's, OCT has been used extensively for biological imaging of tissue structure and function². OCT generates cross-sectional images by measuring echo time delay of backscattered light⁴ by implementing low coherence light source with a fiber-optic Michelson interferometer^{2,4}. SD-OCT, also known as Fourier domain OCT (FD-OCT), was first introduced in 1995⁵ and offers a superior imaging modality compared with traditional time domain OCT (TD-OCT). In SD-OCT, the reference arm is kept stationary resulting in a high speed and ultra high resolution image acquisition⁶⁻⁹.

Presently, TSCW models have been used largely for *in vivo* brain imaging applications of two-photon microscopy in place of a traditional craniotomy. These TSCW have been used concurrently with a custom skull plate or a glass cover slip¹⁰⁻¹³ to provide additional imaging stability. In our studies, we have observed that accessories such as these are not necessary for OCT imaging when a TSCW is used. Therefore, the lack of a skull plate or glass cover slips allows for a wider range of imaging window size as they may interfere with the optical beam and alter OCT images.

A thinned-skull preparation has proven to be advantageous in imaging studies of the brain using two-photon microscopy¹⁰⁻¹³. In our experiments, we utilize a SD-OCT system to image the cortex *in vivo* through a TSCW. Our custom SD-OCT imaging setup contains a broadband, low-coherence light source consisting of two superluminescent diodes (SLD) centered at 1295 nm with a bandwidth of 97 nm resulting in an axial and lateral resolution of 8 μm and 20 μm , respectively¹⁴. With our optical imaging device, we envision that imaging through a TSCW has great potential in identifying and visualizing structures and functions in the optically dense brain tissue.

Protocol

1. Surgical Preparation

1. Female CD 1 mice between the ages of 6-8 weeks were used in our experiments.
2. Anesthetize the mouse with an intraperitoneal injection of a ketamine and xylazine combination (80 mg/kg ketamine/10 mg/kg xylazine). Place the mouse on a homeothermic pad to ensure optimal body temperature at $\sim 37^\circ\text{C}$. Continuously monitor level of anesthesia by testing animal's reflexes (e.g., pinching foot with blunt forceps) and inject more anesthesia when necessary.

- Lubricate both eyes with an artificial tear ointment. Remove hairs on the scalp using a razor and remove residual hair using 70% alcohol prep pads. Apply a thin layer of Nair hair removal cream over the scalp and wait 2 min for it to take effect. Gently wipe away Nair and remaining hair using saline moistened cotton swabs and alcohol prep pads. Scalp should now be completely hairless.
- Disinfect scalp using a betadine swab stick and clean with 70% ethanol prep pads.
- Carefully wrap the animal in surgical drapes to ensure optimal body temperature of $\sim 37^\circ\text{C}$ and mount the animal onto a stereotaxic frame to immobilize the skull. Lightly tap the skull to ensure its stability. A list of materials used is provided in **Table 1**.

2. Thinned-skull Cortical Window Preparation

- Start the incision at the midline point between the eyes. Continue caudally to the midline point between the ears. Part the skin with forceps.
- Locate the area to be thinned under a dissecting microscope and gently remove the fascia using tweezers. Dry the skull with sterile cotton swabs before creating the thinned cortical window. In our experiments, we created a 4×4 mm thinned cranial window ~ 1 mm posterior and lateral to bregma.
- Begin thinning the skull using a round carbide bur with drill bit size 0.75 mm in a surgical hand drill using light sweeping motion only. Do not apply direct pressure onto the skull. Stop drilling every 20-30 sec to remove bone dust using sterile saline and cotton swabs and to avoid overheating the skull. The saline will also aid in dissipating the heat throughout the skull.
- Once the outer layer of the compact bone is completely removed the middle spongy bone layer should now be visible. There may be some slight bleeding as blood vessels are more apparent in the spongy bone layer. Switch to a green stone bur and continue drilling using extra caution as the spongy layer is more delicate. The green stone bur will remove less bone material while creating evenness throughout the cranial window. Stop drilling occasionally to remove bone dust and to cool the skull.
- Finally, when the skull has become more transparent and vasculature on the brain is now visible, begin polishing the skull using a polishing bur. This will allow a more precise thinning while smoothing down the skull. Check thinness of the skull by gently tapping on it with forceps. Stop polishing when the skull becomes slightly flexible.
- The thinned cranial window should now be completely smooth and reflective and ready for imaging (**Figure 1**). Due to the nature of highly scattering tissues of the brain, the skull should be thinned to at least $55\ \mu\text{m}$ for optimal depth penetration. A list of materials used is provided in **Table 1**.

3. Optical Coherence Tomography Imaging

- After surgery is complete, check animal's breathing rate and reflexes to ensure proper level of anesthesia and administer additional anesthesia if necessary. Remove animal from the stereotaxic frame, keep animal wrapped in surgical drapes, and transport animal to the imaging station.
- Before imaging check signs for reflexes and apply additional artificial tear if needed. Mount animal on to the stereotaxic frame to secure the skull.
- Place animal under OCT camera and position the TSCW under the optical beam (**Figure 2**). A cross-sectional view of the skull and brain can now be visualized (**Figure 3**).
- Data acquisition can begin once area of interest is located. For imaging purposes, we use galvo mirrors to achieve an imaging window with a width of 4.0 mm. An imaging depth of 2 mm was obtained with 6 mW of incident power and a focal point 1 mm below the thinned skull. Each cross-sectional area consisted of 2,048 axial scans with an acquisition rate of 0.14 sec per image.
- Volumetric scans of the brain can also be obtained by collecting a series of 2D cross-sectional images by using two sets of galvo mirrors for x-y scanning with the first galvo mirror scanning the beam in the sagittal direction and the second galvo mirror scanning in the coronal direction.

Representative Results

After creating a thinned window over the cerebral cortex the vasculature should now be more visually prominent (**Figure 1**) and will allow for a deeper imaging depth (up to 1 mm). The right cortex is thinned to approximately $55\ \mu\text{m}$ as compared to a normal skull measured at $140\ \mu\text{m}$ (**Figure 1**) and provides greater optical clarity. Further thinning to $10\text{-}15\ \mu\text{m}$ is possible¹¹ however not necessary as the use of glass cover slips and skull plates are not implemented in our experiments (**Figure 1 and 2**). This particular method has allowed us to identify specific structures (cerebral cortex, corpus callosum) in our OCT cross-sectional images (**Figure 3**). Parasagittal OCT images of a normal skull (**Figure 3A**) versus a thinned skull (**Figure 3B**) are shown to compare the outcome of an OCT image with a successful TSCW. Additionally, a coronal cross-sectional OCT image is also obtained to facilitate in identifying midline structures (**Figure 3C**). The maximum signal intensity for **Figure 3** is 45 dB above the noise floor. An intensity profile comparison of a non-thinned skull and a thinned skull reveals a greater signal intensity and depth penetration in a TSCW model (**Figure 4**).

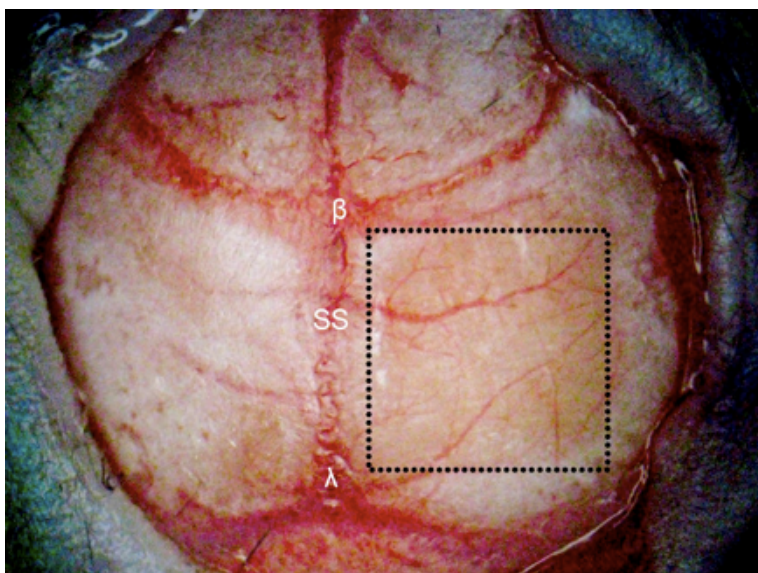


Figure 1. TSCW in a mouse model. A 4 × 4 mm thinned skull window (denoted in the dotted square box) is created ~ 1 mm posterior and lateral to bregma over the right cerebral hemisphere using various dental burs. The right cortex (thinned to approximately 55 μm) is significantly more transparent than the non-thinned skull (left cortex, 140 μm) providing greater depth penetration for optical imaging using OCT. β = bregma, λ = lambda, SS = sagittal suture.



Figure 2. OCT imaging of TSCW *in vivo*. A mouse model with a thinned-skull is fixed in a stereotactic frame under the objective for OCT imaging *in vivo*.

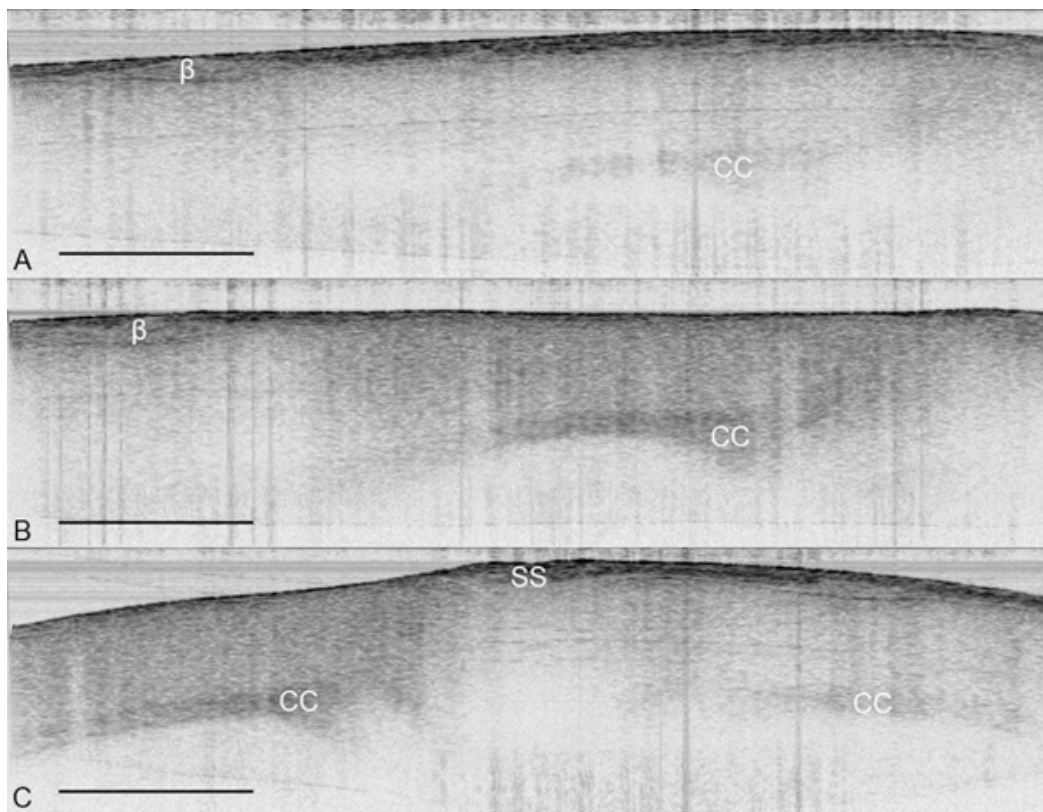


Figure 3. OCT images of the cerebral cortex *in vivo*. (A) Parasagittal OCT image of the cortex under a normal skull. (B) Parasagittal OCT image of the cortex under a thinned skull. (C) Coronal OCT image of a thinned skull (left) and a normal skull (right). The structures of the brain are more visually apparent under a TSCW as compared to a normal skull. OCT images from were obtained from the same mouse *in vivo* with imaging size 5.5 mm × 2 mm with maximum signal intensity of 45 dB. β = bregma, CC = corpus callosum, SS = sagittal suture, scale bar = 1 mm.

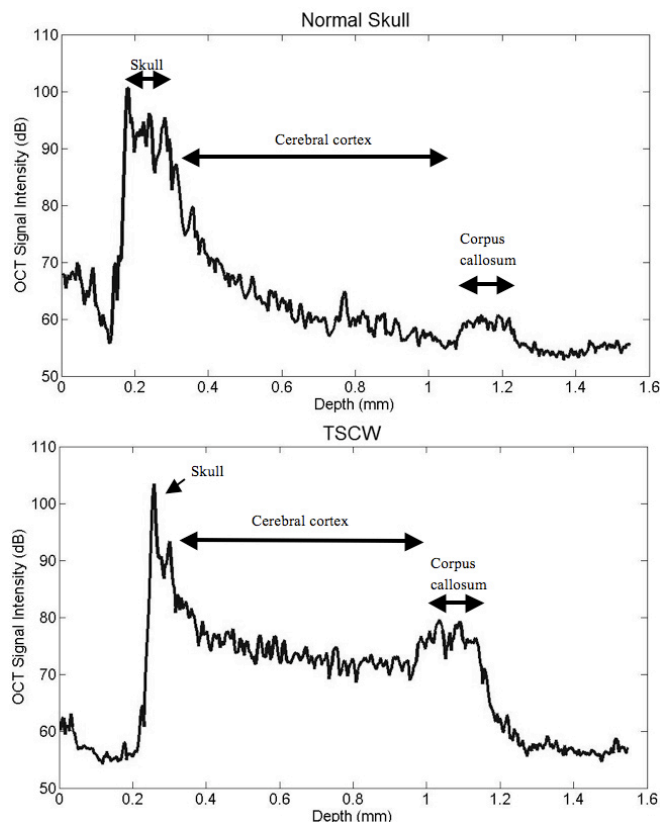


Figure 4. Intensity profile comparisons of normal and thinned skull prep. TSCW permits increased signal intensity and depth penetration. The TSCW achieves an imaging depth of about 1 mm with sufficient SNR.

Discussion

Imaging with OCT and a thinned-skull is a novel neuro-imaging technique that has only been recently investigated^{15, 16}. In our experiments, we demonstrated the feasibility of SD-OCT imaging through a TSCW in a mouse model *in vivo*. From our results, the skull is thinned to approximately 55 μm and the penetration depth is obtained at approximately 1 mm with image resolution of 8 μm and 20 μm in the axial and lateral direction, respectively. In the signal intensity profile, OCT imaging through a TSCW increases the signal intensity and depth penetration as compared to a normal skull (**Figure 4**). In comparison, two-photon imaging with a TSCW at skull thickness of ~10-15 μm can reach imaging depths of 150-250 μm below pial surface^{10, 11, 13} with axial resolution at ~3 μm ¹⁰ while a thinned skull of ~20 μm imaging depth can reach up to 300-400 μm within the cerebral cortex¹². Overall, optical imaging with OCT proves to be a promising imaging modality, permitting a thicker TSCW during the thinning process while providing deeper depth penetration than multiphoton microscopy.

Utilizing a thinned-skull is advantageous in optical imaging such as OCT^{15, 16} and two-photon microscopy¹⁰⁻¹³ as it provides little to no neuroinflammation as compared to a craniotomy if thinning is conducted successfully^{11, 12, 15, 16}. Employing a craniotomy for imaging may result in reactive microglia as well as upregulation of glial fibrillary acidic protein (GFAP) in reactive astrocytes after insults to the brain. However, imaging after adopting a thinned-skull technique reveals non-active microglia and weak GFAP immunostaining implying non-reactive astrocytes¹⁰. Through proper thinning of the skull, specific structures within the cerebral cortex, such as microglia morphology and cortical vasculature, can be distinguished¹¹⁻¹³. Nevertheless, there are drawbacks of using a TSCW for optical imaging. If the skull is not thinned to the correct thickness or the skull has rough surfaces due to improper thinning depth penetration for imaging may be limited. Another downside for poor imaging depth may result from sub-dural hemorrhage due to vibrations of drilling. Bleeding underneath the dura is unavoidable and therefore cannot be used for OCT imaging. In cases such as these, a new animal model should be used for the experiment.

Identifying certain structures within the cortex using OCT through a TSCW can be helpful in tracking neurodegenerative diseases and in studying changes in brain function. Imaging blood flow can be achieved through Doppler OCT^{17, 18} as quantifying cerebral blood flow is paramount in monitoring the metabolic demands of the brain in studying stroke, Alzheimer's disease¹⁸, or brain tumors¹⁷. Axonal and neuronal degeneration is also prominent in OCT images and can benefit studies of various brain disorders. By imaging the retinal nerve fiber layer (RNFL), which contains ganglion cell axons, mechanisms of neuro-degeneration, neuro-protection, and neuro-repair can be visualized not only in optical disorders but also in neurological diseases such as Parkinson's¹⁹ and multiple sclerosis^{20, 21}, the latter which has been explored in detail by measuring the macula²¹ and retinal layer thickness through OCT segmentation techniques²⁰.

Neuro-imaging with OCT is not only restricted to imaging structures and functions of the brain. OCT can be advantageous in chronic *in vivo* imaging^{10, 11} as well as in stereotactic procedures such as electrophysiological and microinjection studies^{1, 3, 15-17}. In neurosurgery, OCT can be used as a biopsy or guiding tool² by allowing surgeons to view real-time feedback images of specific anatomical features within the brain¹⁷. With further developments, we believe our current combination of SD-OCT with a TSCW has the potential to improve a clinician's ability to diagnosis neurological deficits when it is applied with other modalities such as an intracranial pressure (ICP) monitor²², magnetic resonance imaging (MRI), or computerized axial tomography (CAT)¹.

Disclosures

No conflicts of interest declared.

Acknowledgements

This work was supported by the UC Discovery Proof of Concept grant and by the NIH (R00 EB007241). The authors would also like to thank Jacqueline Hubbard for her assistance in this experiment.

References

1. Bizheva, K., Unterhuber, A., Hermann, B., Povazay, B., Sattmann, H., & Drexler, W. Imaging *ex vivo* and *in vitro* brain morphology in animal models with ultrahigh resolution optical coherence tomography. *Journal of Biomedical Optics*. **9**, 719-724 (2004).
2. Fujimoto, J.G. Optical coherence tomography for ultrahigh resolution *in vivo* imaging. *Nature Biotechnology*. **21**, 1361-1367 (2003).
3. Wantanabe, H., Rajagopalan, U.M., Nakamichi, Y., Igarashi, K.M., Kadono, H., & Tanifuji, M. Swept source optical coherence tomography as a tool for real time visualization and localization of electrodes used in electrophysiological studies of brain *in vivo*. *Biomedical Optics Express*. **2**, 3129-3134 (2011).
4. Huang, D., Swanson, E.A., Lin, C.P., Schuman, J.S., Stinson, W.G., Chang, W., Hee, M.R., Flotte, T., Gregory, K., Puliafito, C.A., & Fujimoto, J.G. Optical coherence tomography. *Science*. **254**, 1178-1181 (1991).
5. Mitsui, T. Dynamic range of optical reflectometry with spectral interferometry. *Japanese Journal of Applied Physics*. **38**, 6133-6137 (1999).
6. de Boer, J.F., Cense, B., Park, B.H., Pierce, M.C., Tearney, G.J., & Bouma, B. Improved signal-to-noise ratio in spectral-domain compared with time-domain optical coherence tomography. *Optics Letters*. **28**, 2067-2069 (2003).
7. de Boer, J.F. In: *Optical Coherence Tomography: Technology and Applications*, Ch. 5, Springer, (2008).
8. Choma, M.A., Sarunic, M.V., Yang, C., & Izatt, J.A. Sensitivity advantage of swept source and fourier domain optical coherence tomography. *Optics Express*. **11**, 2183-2189 (2003).
9. Leitgeb, R.A., Drexler, W., Unterhuber, A., Hermann, B., Bajraszewski, T., Le, T., Stingl, A., & Fercher, A.F. Ultrahigh resolution fourier domain optical coherence tomography. *Optics Express*. **12**, 2156-2165 (2004).
10. Drew, P.J., Shih, A.Y., Driscoll, J.D., Knutsen, P.M., Blinder, P., Davalos, D., Akassoglou, K., Tsai, P.S., & Kleinfeld, D. Chronic optical access through a polished and reinforced thinned skull. *Nature Methods*. **7**, 981-984 (2010).
11. Shih, A.Y., Mateo, C., Drew, P.J., Tsai, P.S., Kleinfeld, D. A Polished and Reinforced Thinned-skull Window for Long-term Imaging of the Mouse Brain. *J. Vis. Exp.* (61), e3742, doi:10.3791/3742 (2012).
12. Yang, G., Pan, F., Parkhurst, C.N., Grutzendler, J., & Gan, W. Thinned-skull cranial window technique for long-term imaging of the cortex in live mice. *Nature Protocols*. **5**, (2010).
13. Marker, D.F., Tremblay, M., Lu, S., Majewska, A.K., & Gelbard, H.A. A Thin-skull Window Technique for Chronic Two-photon *In vivo* Imaging of Murine Microglia in Models of Neuroinflammation. *J. Vis. Exp.* (43), e2059, doi:10.3791/2059 (2010).
14. Wang, Y., Oh, C.M., Oliveira, M.C., Islam, M.S., Ortega, A., & Park, B.H. GPU accelerated real-time multi-functional spectral-domain optical coherence tomography system at 1300nm. *Optics Express*. **20**, 14797-14813 (2012).
15. Aguirre, A. D., Chen, Y., & Fujimoto, J.F. Depth-resolved imaging of functional activation in the rat cerebral cortex using optical coherence tomography. *Opt. Lett.* **31**, 3459-3461 (2006).
16. Chen, Y., Aguirre, A.D., Ruvinskaya, L., Devor, A., Boas, D.A., & Fujimoto, J.G. Optical coherence tomography (OCT) reveals depth-resolved dynamics during functional brain activation. *Journal of Neuroscience Methods*. **178**, 162-173 (2009).
17. Liang, C., Wierwille, J., Moreira, T., Schwartzbauer, G., Jafri, M.S., Tang, C., & Chen, Y. A forward-imaging needle-type OCT probe for image guided stereotactic procedures. *Opt Express*. **19**, 26283-26294 (2011).
18. Srinivasan, V.J., Sakadzic, S., Gorczynska, I., Ruvinskaya, S., Wu, W., Fujimoto, J.G., & Boas, D.A. Quantitative cerebral blood flow with optical coherence tomography. *Optics Express*. **18**, 2477-2494 (2010).
19. Galetta, K.M., Calabresi, P.A., Frohman, E.M., & Balcer, L.J. Optical Coherence Tomography (OCT): imaging the visual pathway as a model for neurodegeneration. *The Journal of the American Society for Experimental NeuroTherapeutics*. **8**, 117-132 (2011).
20. Seigo, M.A., Sotirchos, E.S., Newsome, S., Babiarz, A., Eckstein, C., Ford, E., Oakley, J.D., Syc, S.B., Frohman, T.C., Ratchford, J.N., Balcer, L.J., Frohman, E.M., Calabresi, P.A., & Saidha, S. *In vivo* assessment of retinal neuronal layers in multiple sclerosis with manual and automated optical coherence tomography segmentation techniques. *J. Neurol.*, (2012).
21. Frohman, E.M., Fujimoto, J.G., Frohman, T.C., Calabresi, P.A., Cutter, G., & Balcer, L.J. Optical coherence tomography: a window into the mechanisms of multiple sclerosis. *Nature Clinical Practice*. **4**, 664-675 (2008).
22. Gill, A.S., Rajneesh, K.F., Owen, C.M., Yeh, J., Hsu, M., & Binder, D.K. Early optical detection of cerebral edema *in vivo*. *J. Neurosurg.* **114**, 470-477 (2011).